Economic Geology
Vol. 93, 1998, pp. 896–910

Basinal Fluid Flow Models Related to Zn-Pb Mineralization in the Southern Margin of the Maritimes Basin, Eastern Canada*

GUOXIANG CHI[†] AND MARTINE M. SAVARD

Geological Survey of Canada, Quebec Geoscience Centre, 2535 Boulevard Laurier, P.O. Box 7500, Sainte-Foy, Quebec, Canada G1V 4C7

Abstract

The carbonate-hosted Zn-Pb deposits in the Lower Windsor Group, Nova Scotia, are located along the southern margin of the Maritimes basin. Previous studies suggest that the deposits formed from basinal brines expelled from the basal part of the Maritimes basin (Horton Group), possibly related to tectonic events in late stages of the basin history, but it remains unclear where the specific source regions were and which mechanism is responsible for fluid expulsion from the source regions to the sites of mineralization. This paper presents two numerical models to address these problems. The first model, based on a stratigraphic profile ranging from the center to the southern margin of the Maritimes basin, simulates the distribution and evolution of fluid overpressures due to sediment compaction. The second model simulates the temperature distribution in a marginal sub-basin under the assumption that fluid flow was driven by topographic relief related to an uplift (highlands) proximal to the ore deposits.

Modeling of fluid overpressure evolution indicates that, if the Horton Group sediments were laterally confined by basement highs or faults, fluid pressures approaching or exceeding loading pressures would be easily built up within the Horton Group after deposition of the overlying Windsor evaporites. Strong overpressures in the Horton Group rocks are predicted not only in the central part of the Maritimes basin but also in shallower sub-basins close to the sites of mineralization. In contrast, if the Horton Group rocks are assumed to be laterally continuous across the Maritimes basin, fluid pressures in the Horton Group would remain near hydrostatic and strong overpressures would be built up only within the evaporite layer. In both cases, the geothermal gradients would not be significantly disturbed by the sediment compaction-driven fluid flow.

Modeling of topography-driven flow indicates that the geothermal gradients are only slightly disturbed if rock permeabilities are inherited from the compaction model but could be strongly disturbed if higher permeabilities are assigned to the basal aquifer, and high-permeability zones (conduits) are assumed to cut through the evaporite layer and link the highlands (recharge area), basal aquifer, and discharge area. The temperature at the site of mineralization could be increased relative to the background temperature, but under steady-state conditions it could not have reached the ca. 250°C indicated by fluid inclusions in the deposits. Such high temperatures could be reached transiently if the conduits and basal aquifer had permeabilities higher than about 0.1 D.

The numerical modeling results suggest that sediment compaction-driven fluid flow could not have been responsible for mineralization because it cannot satisfy the thermal conditions at the deposits. Topography-driven flow may satisfy the thermal conditions at the deposits under the assumption of high-permeability conduits and a basal aquifer. Whether or not such conditions existed in the southern margin of the Maritimes basin needs further study. Based on the modeling results of fluid overpressure development, we favor a model in which the main-stage ore-forming fluids were derived from the basal part of individual sub-basins proximal to the deposits and were driven by sudden release of overpressures, probably triggered by tectonic events. Topography-driven flow may have been dominant in the postore stage, i.e., after the dissipation of overpressures. This model agrees with other geochemical studies that indicate separate source regions for different deposits, high fluid flow rates, and involvement of lower salinity fluids after the main-stage mineralization.

Introduction

THE ORIGIN of the carbonate-hosted Zn-Pb-Ba deposits in the Lower Windsor Group in Nova Scotia, located along the southern margin of the Maritimes basin (Fig. 1), has been attributed to basinal brines expelled from the basal part of the basin fill (the Horton Group; e.g., Ravenhurst and Zentilli, 1987; Ravenhurst et al., 1989; Sangster and Savard, 1994; Chi et al., 1998; Sangster et al., 1998; Savard and Kontak, 1998). However, it remains unclear where the specific source regions were and how the fluids were expelled from the source regions to the sites of mineralization. Two hydrodynamic models have been previously proposed. One suggested that sudden release of overpressured fluids from the central (deepest) part of the Maritimes basin, about 100 to 150 km away from the ore deposits, was responsible for mineralization (the distal source-overpressure model; Ravenhurst and Zentilli, 1987; Ravenhurst et al., 1989). The other model suggested that fluid flow was driven by topographic relief related to uplifts close to the deposits (<60 km) and implied that the ore-forming fluids originated from nearby sub-basins (the proximal source-gravity model; Sangster and Savard, 1994). The key constraint on both models is the high fluid temperatures (ca. 250°C) indicated by fluid inclusions at the deposits, more than 100°C higher than the background temperatures in the host rocks (Chi et al., 1998). The distal source-overpressure model can easily satisfy the thermal condition in the inferred source region but faces the difficulty of maintaining overpressures to drive fluids across half the basin which is character-

* Geological Survey of Canada Contribution 1996148.
† Corresponding author: email, gchi@gsc.nrcan.gc.ca

0361-0128/98/2005/896-15$6.00

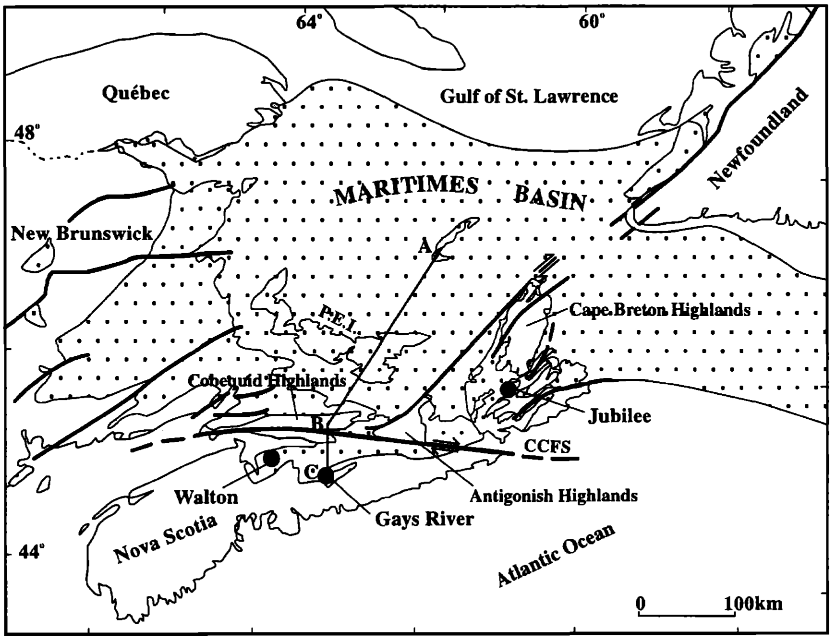

FIG. 1. The scope of the Maritimes basin and its major structures (modified from St. Peter, 1993). Line A-B-C indicates the position of the model cross section shown in Figure 3. CCFS = Cobequid-Chedabucto fault system.

ized by horst and graben structures. The proximal source-gravity model can satisfy the thermal condition in the source regions when a higher geothermal gradient is applied (Chi et al., 1998) but remains to be examined as to whether the fluids could be efficiently conveyed to the sites of mineralization with minimum temperature decrease.

This paper presents two numerical models to address the fluid flow and source problems outlined above, using a numerical technique developed by Bethke (1985). The first model, based on a stratigraphic profile ranging from the center to the southern margin of the Maritimes basin, simulates the evolution of fluid pressure, temperature, and fluid flow rate during the sedimentation history of the basin. The purpose of this model is to see whether or not strong fluid overpressures could have been built up in the Horton Group sediments by the time of mineralization, and how they might have been distributed (central part of the basin versus marginal sub-basins). The second model is based on a stratigraphic profile ranging from an uplift (the Cobequid highlands) to the site of a deposit (Gays River). This model assumes that fluid overpressures due to sediment compaction had been somehow dissipated by the time of mineralization and that fluid flow was driven by topographic relief imposed by the highlands. The purpose of this model is to evaluate whether or not topographic relief could have driven fluids from the sub-basins south of the highlands to the sites of mineralization without losing much heat, i.e., whether the high fluid temperatures in the deposits can be explained by topography-driven flow as proposed elsewhere (Garven and Freeze, 1984; Garven et al., 1993). The implications of the numerical modeling results on ore genesis will be discussed considering the geologic and geochemical characteristics of the deposits.

Sedimentary and Tectonic History of the Maritimes Basin and Timing of Mineralization

The Maritimes basin is a late Paleozoic intracontinental successor basin developed upon the Acadian basement. It occupies a large area (>250,000 km^2) in New Brunswick, Nova Scotia, Newfoundland, and the Gulf of St. Lawrence (Fig. 1) and comprises a thick (up to 12 km in the central part) sequence of Late Devonian to Early Permian continental and marine sediments (Fig. 2).

From the Middle Devonian to early Viséan, continental clastic sediments of the Fountain Lake (Middle to Late Devonian) and Horton (Late Devonian to early Viséan) Groups (Ryan et al., 1991) were deposited, first, in fault-bounded basins, and then, as laterally extensive thin veneers in sag basins (Durling and Marillier, 1993). In this paper, we follow Howie and Barss (1975) and use the term Horton Group for all the rocks lying between the Acadian basement and the Windsor Group rocks. The lithology of the Horton Group varies from place to place. In the type section, the lower part of the Horton Group (the Horton Bluff Formation) consists of gray to brownish feldspathic conglomerate, quartzitic sandstone, siltstone and shale, and rare, thin, lenticular limestone; the upper part of the Horton Group (the Cheverie Formation) consists of red and gray, arkosic and feldspathic conglomerate, red and minor gray sandstone, siltstone, and shale (Howie and Barss, 1975). A lithologic sequence reflecting the general profile of the Horton Group in the Maritimes basin was described by Kelley (1970, see Howie and Barss, 1975) as sandstone and conglomerate succeeded by siltstone, sandstone, and shale, then by sandstone, siltstone, and conglomerate. A similar lithologic sequence was also described by Martel and Gibling (1996) and Hamblin (1992) and was broadly reflected in the restored basinal-scale stratigraphic sections

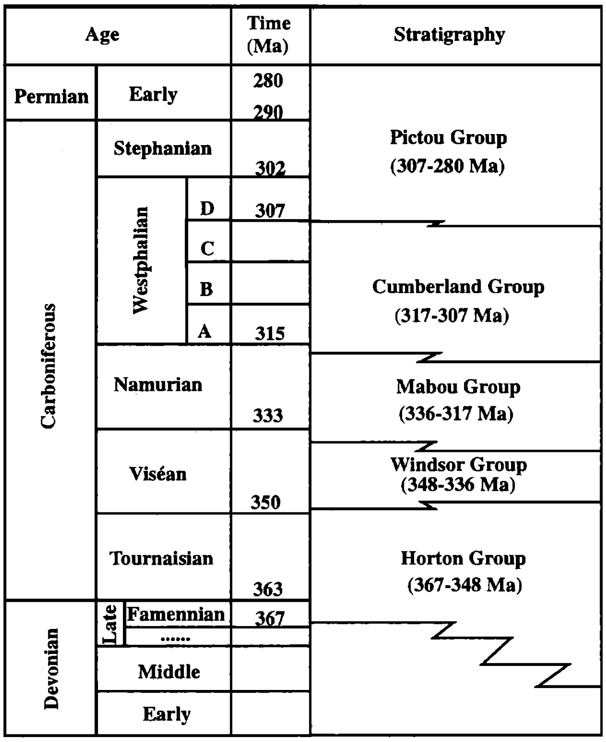

FIG. 2. Stratigraphic divisions and approximate time scales of the Maritimes basin (compiled from Ryan et al., 1991 and St. Peter, 1993).

of Howie and Barss (1975), where the Horton Group was divided into four layers: i.e., in ascending order, conglomerate, sandstone, shale, and siltstone. The lower two layers pinch out at basement highs or are bounded by faults, whereas the upper two layers are laterally continuous. According to the isopach map of Howie and Barss (1975), the Horton Group is thickest (>4 km) in the central part of the Maritimes basin (around the Magdalen Islands) and generally becomes thinner toward the margin of the basin, but it can be fairly thick in some sub-basins in the southern margin of the basin, e.g., the River Denys sub-basin on Cape Breton Island (>3 km), and the St. Mary's sub-basin (maximum about 3.5 km; Murphy et al., 1994).

In late Tournaisian time, a tectonic event, indicated by an unconformity or disconformity between the Horton Group and the overlying Windsor Group, affected part of the basin, resulting in folding, faulting, and erosion of the Horton Group rocks (St. Peter, 1993). From the early to late Viséan, a sequence of marine sediments that become the Windsor Group were deposited over the whole Maritimes basin area. At the beginning of this marine transgression, a thin layer of fine-grained limestone known as the Macumber Formation overlaid the Horton Group rocks. Locally, carbonate banks formed on top of basement highs (e.g., the Gays River Formation). This carbonate unit was succeeded by a thick sequence of evaporites with intercalated carbonates developed in a shallow, fluctuating, marine environment. With the gradual withdrawal of the Windsor sea, a sequence of clastics and carbonates with increasing continental components was deposited. According to the isopach map of Howie and Barss (1975), the Windsor Group is generally thickest in the central part of the Maritimes basin (>5 km) and becomes gradually thinner toward the margin of the basin.

From the late Viséan to late Westphalian, sedimentation took place in continental environments and was mainly concentrated in depocenters. This was partly responsible for the complexity and variety of stratigraphic divisions and the nomenclature of the post-Windsor strata. In this paper, we use the nomenclature of Ryan et al. (1991) which was based on detailed stratigraphic studies in the Cumberland sub-basin. From the late Viséan to late Namurian, sedimentation was fairly slow; sediments (belonging to the Mabou Group, previously the Canso Group) were mainly fine-grained sandstone and mudstone. In late Namurian time, a tectonic event took place, as indicated by an unconformity or disconformity between the Cumberland Group and older rocks (St. Peter, 1993). From the late Namurian to Westphalian C, some areas were subject to rapid uplifting, resulting in highlands (e.g., the Cobequid highlands) and adjacent depocenters (e.g., the Cumberland sub-basin). Sedimentation was so rapid in some depocenters that trees were preserved in upright position (Howie and Barss, 1975). The sediments of this period belong to the Cumberland Group, which includes, at its base, sediments previously assigned to the Riversdale Group, and at its top, part of the sediments previously assigned to the Pictou Group (Ryan et al., 1991). The lithology varies from pebble and boulder conglomerate, to sandstone, to mudstone, and to coal seams. Large-scale detachment faulting, as documented by Lynch and Tremblay (1994) on Cape Breton Island, probably took place in this period. On the other hand, compressional structures probably developed in some parts of the basin (e.g., the Athol syncline in the Cumberland sub-basin, Reed et al., 1993).

Between Westphalian C and D, a major tectonic event is indicated by an unconformity or disconformity between the Pictou Group and preexisting rocks (St. Peter, 1993). Strong deformation took place along master faults (e.g., the Cobequid-Chedabucto fault system, see Fig. 1) and adjacent areas. From Westphalian D to the Early Permian, a sequence of nonmarine conglomerate, sandstone, shale, and coal seams belonging to the Pictou Group was deposited. It represents a transgressive sequence which spreads laterally over all older rocks except in its later stage.

The Zn-Pb-Ba deposits on the southern margin of the Maritimes basin are hosted by the carbonate rocks of the Lower Windsor Group (the Macumber Formation and equivalent Gays River Formation). All the deposits are epigenetic, comprising replacement and open-space-filling ores, i.e., they were formed after the host rocks (Viséan) (Graves and Hein, 1994). Whole-rock $^{39}Ar/^{40}Ar$ dating of one of the deposits, Gays River, indicates a mineralization age of 297 ± 27 Ma (Kontak et al., 1994). This age is broadly consistent with earlier estimates by a paleomagnetic method (300–320 Ma, Pan et al., 1993) and by the fission-track method on zircon as well as the K-Ar method on clays (ca. 320 Ma, Ravenhurst et al., 1989). Clay samples separated from Horton rocks at Upper Brookside (near the Cobequid-Chedabucto fault system) gave an Rb-Sr isochron age of 300 ± 6 Ma (Ravenhurst et al., 1989), which is interpreted to be the age of basinal brine flow related to mineralization (Ravenhurst et al., 1989).

This age, and the age of the Gays River deposit, broadly coincides with the tectonic event indicated by the unconformity between Westphalian C and D (ca. 307 Ma). The other deposits have not been dated, but they may be related to the tectonic events in the late Carboniferous and may have ages similar to those of the Gays River deposit.

Modeling of the Distribution and Evolution of Fluid Overpressure

Model representation of the basin cross section

The modeling of fluid pressure requires the establishment of a physical model describing basin geometry, lithologies, and sedimentation rates. We have used a two-dimensional model (Fig. 3) which starts at the center of the Maritimes basin (near the Magdalen Islands in the Gulf of St. Lawrence), extends southwestward to the Cobequid highlands, then turns southward, and ends near the Gays River deposit (line A-B-C in Fig. 1). The model cross section is mainly based on a series of isopach maps and restored stratigraphic sections of Howie and Barss (1975), with the post-Windsor divisions being modified according to the nomenclature of Ryan et al. (1991). Modifications were also made for the southern part of the section by taking into consideration the stratigraphic data of Giles and Boehner (1982) and Murphy et al. (1994). One of the uncertainties about this profile is that different parts of the basin, separated by major faults, may have moved with respect to each other during and after the formation of the basin. For example, Keppie (1982) estimated that the Cobequid-Chedabucto fault system south of the Cobequid highlands (Fig. 1) probably underwent a dextral movement of approximately 165 km during the late Westphalian to Permian Hercynian orogeny, and a sinistral movement of about 75 km during the Triassic. This means that the block south of the Cobequid-Chedabucto fault system was situated 90 km east of its present position before the dextral movement along the fault was moved westward (relative to the block north of the fault) to 75 km west of its present position by the end of the dextral movement, and then was moved eastward to its present position during the Triassic. The timing and scale of these movements, however, are not well constrained by stratigraphic data (Keppie, 1982), and it is difficult to trace the relative position between the blocks north and south of the Cobequid-Chedabucto fault system through time. In particular, the position of the ore deposits relative to the block north of the fault at the time of mineralization is difficult to determine because the mineralization possibly took place during the inferred dextral movement along the fault system. Therefore, the present-day position (line A-B-C in Fig. 1) is used in the construction of the model cross section. This simplification, however, does not change the overall structures in this part of the Maritimes basin. Given the structural complexity of the basin, no single cross section can comprehensively represent the variation of basin geometry and lithologies in all directions, and the model section was constructed in the spirit of outlining the most important sedimentary and structural features of the southern part of the Maritimes basin.

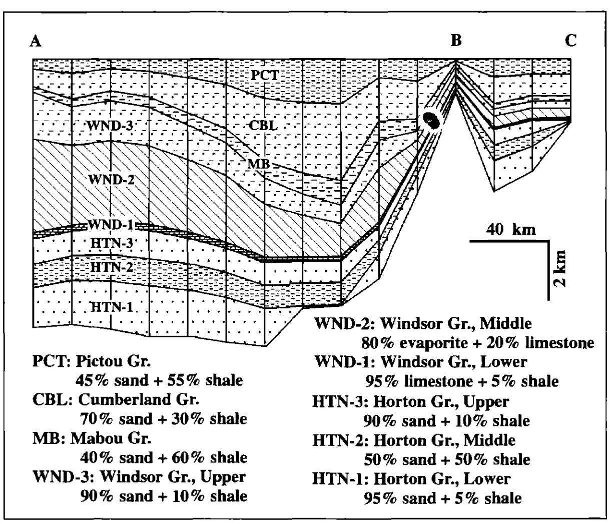

FIG. 3. Model cross section used in modeling the distribution and evolution of fluid overpressures during the sedimentation history of the Maritimes basin (the positions of A, B, and C are shown in Fig. 1). The thicknesses of the various units are based on a series of isopach maps and restored stratigraphic sections of Howie and Barss (1975), with modifications being made for the southern part of the section by taking into consideration the stratigraphic data of Giles and Boehner (1982) and Murphy et al. (1994). The lithologic approximations of the units are based on stratigraphic data of Howie and Barss (1975), Hacquebard (1986), Martel and Gibling (1996), Lavoie (1994), and Ryan and Boehner (1994). The section shown is that in Early Permian times.

The Horton Group is divided into three hydrogeologic units. The lower unit corresponds to the conglomerate and sandstone layers in the cross sections of Howie and Barss (1975) , the middle unit to their shale layer, and the upper unit to their siltstone layer. The lower unit of the Horton Group pinches out at basement highs. The Windsor Group is also divided into three units in the model profile: a lower unit representing the first marine carbonates (the Macumber-Gays River Formations), a middle unit comprising mainly evaporites, and an upper unit comprising mainly siltstone. For the rest of the stratigraphy, each group (Mabou, Cumberland, and Pictou) is represented by a single hydrogeologic unit. The lithologic approximations of each unit, based on stratigraphic data of Howie and Barss (1975), Hacquebard (1986), Lavoie (1994), Ryan and Boehner (1994), and Martel and Gibling (1996), are presented in Figure 3. No lateral variations in lithology were considered within individual stratigraphic units in the model. The absolute ages of group boundaries, shown in Figure 2 and used for calculating sedimentation rate, were mainly adopted from St. Peter (1993).

Governing equations and numerical procedures

The spatial distribution and temporal evolution of fluid pressure, temperature, and fluid flow velocity during sedimentation and compaction were obtained by numerically solving the medium continuity, fluid continuity, and heat conservation equations (eqs A1–A3, Appendix) described by the mathematical model of Bethke (1985, 1986). The model cross section was broken up into a series of nodal blocks which are described in terms of a curvilinear coordinate system: the x coordinate is parallel to the bedding and the z coordinate is vertical. The governing equations were converted to a finite difference form in the curvilinear coordinate system and solved for each nodal point in the center of a nodal block. The numerical solution procedure used in this study is similar to that described by Bethke (1985), except that the alternating direction implicit (ADI) method (see Jaluria and Torrance, 1986) is used instead of the band matrix direct method. The ADI method gives rise to tridiagonal matrices for the two alternating directions and the computation scheme is very efficient. The source code was written in FORTRAN and run on a PC-486 computer. Application of the source code to simplified problems shows excellent agreement between numerical results and analytical solutions (Kakac and Yener, 1985). The source code was also tested against the model of Bethke (1985), whose program BASIN2 has been widely used in petroleum applications (e.g., Harrison and Summa, 1991; Kaufman, 1994). The two sets of results compare very well.

The numerical solution starts with the following initial conditions: a layer of Horton Group sediments (<600 m) is in a hydrostatic state (i.e., overpressure = 0; definition of overpressure is given in eq. A4 in the Appendix) and the temperature is controlled by heat conduction. A thin layer of sediment is added to the top of previous sediments with each time step, and all sediments subside according to the rule described by the medium continuity equation. For a given time step, the medium continuity equation is first solved to obtain the settling velocities and porosities of the medium, which are then used to solve the fluid flow equation to obtain fluid overpressures. Since porosity is dependent on effective depth, which is in turn dependent on fluid overpressure (see below), the medium continuity equation has to be recalculated by using the last overpressure values. Iteration between the medium continuity and fluid flow equations continues until the porosity values are convergent ($|(\phi^{k+1}-\phi^{k})/\phi^{k+1}|/<10^{-3}$). The numerical solution then proceeds to solve the heat transfer equation to obtain temperature values. When all three equations are solved, a new time step starts, and so on. A new layer of nodal blocks is created when a target thickness is reached. A total of 1,360 time steps and 71 layers of nodal blocks were used in the calculation. With 15 vertical grid lines (20 km apart from each other; see Fig. 3), this corresponds to a total of 1,065 finite difference nodal blocks.

Rock and fluid properties and boundary conditions

Rock and fluid properties used in numerical calculations are listed in Table 1. Because the compositional evolution of the fluid is not modeled, the fluid is approximated by fresh water for simplicity. The viscosity, coefficient of thermal expansion, coefficient of compressibility, heat capacity, and heat conductivity of the fluid were all assumed to be constant, and the density of the fluid was approximated as a function of temperature and pressure (Bethke, 1985). The density, heat capacity, and thermal conductivity of the solid matrix were assumed to be constant (Bethke, 1985; Garven, 1985). The enthalpy of the fluid was approximated by heat capacity multiplied by temperature based on the data compiled by Phillips et al. (1981). The thermal conductivity of the fluid-saturated medium was calculated as the geometric mean of the solid matrix and the fluid (Raffensperger and Garven, 1995). Porosities (ϕ) of sediments are calculated as a function of effective depth (z_e):

$$\phi = \phi_0 e^{-z_e b} + \phi_1 \tag{1}$$

where ϕ_0 is porosity at deposition, ϕ_1 is irreducible porosity, and b is an empirical parameter (Kaufman, 1994). The effective depth (z_e) is defined as:

$$z_e = z - \frac{\Phi - \Phi_{sc}}{(\rho_{sm} - \rho_w)g} \tag{2}$$

where z is depth, Φ is fluid overpressure, sc denotes surface conditions, ρ_w and ρ_{sm} are constant densities of water and water-saturated sediments, respectively, and g is gravity (Bethke, 1985; Harrison and Summa, 1991). Permeability is related to porosity by the expression:

$$\log k_x = A\phi + B \tag{3}$$

where k_x is horizontal permeability, and A and B are lithology-dependent constants (Bethke, 1985; Harrison and Summa, 1991; Kaufman, 1994). The lithology-dependent constants ϕ_0, ϕ_1, b, A and B, as well as the ratios of horizontal to vertical permeabilities which are used in this study, are listed in Table 2. The parameters for the porosity-effective depth relation (eq. 1) are adopted from Kaufman (1994). They differ from those used by Harrison and Summa (1991) in that an irreducible porosity is assumed. Since sediment compaction is modeled as an irreversible process in this study, i.e., porosity, once reduced, will not increase when fluid overpressure increases, the assumption of an irreducible porosity is preferred. A sensitivity study indicates that the use of the porosity

TABLE 1. Rock and Fluid Properties Used in Numerical Calculations

Property	Value		Reference
Fluid			
Density	$\rho = 1.0 \times 10^{+3} \exp[\beta P - \alpha(T - 25)]$	(kg/m^3)	(1)
Viscosity	$\mu = 1.0 \times 10^{-3}$	(kg/m/s or Pa·s)	(1)
Thermal expansion coefficient	$\alpha = 5.0 \times 10^{-4}$	(/°C)	(1)
Compressibility coefficient	$\beta = 4.3 \times 10^{-10}$	(m·s^2/kg or /Pa)	(1)
Heat capacity	$C_f = 4.2 \times 10^{+3}$	(J/kg/°C)	(1)
Heat conductivity	$K_f = 0.63$	(W/m/°C)	(2)
Solid matrix			
Density	$\rho_r = 2.7 \times 10^{+3}$	(kg/m^3)	(1)
Heat capacity	$C_r = 0.84 \times 10^{+3}$	(J/kg/°C)	(1)
Heat conductivity	$K_r = 2.5$	(W/m/°C)	(2)

References: (1) Bethke (1985); (2) Garven (1985).

TABLE 2. Constants Related to Porosity and Permeability Calculations

Lithology	ϕ_0	ϕ_1	b	A	B	k_x/k_z
Sandstone	0.40	0.10	0.50	15	−3	2.5
Shale	0.55	0.05	0.85	8	−8	10
Platform limestone	0.40	0.05	0.55	6	−4	2.5
Reef limestone	0.40	0.10	0.55	15	−3	2.5
Evaporites	0.50	0.05	10.00	8	−8	10

° b is in km^{-1}, permeability calculated from A and B is in darcies

parameters of Harrison and Summa (1991) tends to produce slightly higher fluid overpressures. The parameters for the permeability-porosity relation (eq. 2) are adopted from Harrison and Summa (1991) for sandstone and shale, which are based on porosity and permeability data for the Gulf of Mexico basin, and from Kaufman (1994) for limestones and evaporites. The ratio of horizontal to vertical permeabilities for evaporites is assumed to be the same as that for shale. Variational studies indicate that fluid overpressure values are insensitive to sandstone permeability but are sensitive to shale and evaporites permeabilities (see also Harrison and Summa, 1991). Since we have not considered the influence of dehydration of clay minerals and probably gypsum (Ravenhurst and Zentilli, 1987) on fluid overpressures, the parameters listed in Table 2 are probably conservative. Porosities of mixed rock types were calculated as an arithmetic mean of the porosities of the end members. Vertical permeabilities were calculated using a harmonic mean for all lithologic combinations (Harrison and Summa, 1991). Horizontal permeabilities were calculated in two ways in conjunction with different pinch-out assumptions (see later): as a geometric mean, and as an arithmetic mean for all lithologic combinations except for the middle unit of the Windsor Group (geometric mean).

The basement heat flux used in the model (110 mW/m^2) is inferred from paleogeothermal gradients (most likely > 65°C/km) near the time of mineralization (Chi et al., 1998). This value is very high in comparison with that of most sedimentary basins but is possible for the tectonic regime of the Maritimes basin (Chi et al., 1998). In addition, it has been known that many of the Devonian age granites in Nova Scotia, e.g., the South Mountain batholith (Chatterjee and Muecke, 1982) south of the Maritimes basin, are high heat production granites. Such granites, if present in the basement underneath the Maritimes basin, could have been an important heat source. In fact, a higher paleogeothermal gradient (>80°C/km) has been indicated by the vertical variation of vitrinite reflectance (R_o) values along a deep drill core in the center of the Shubenacadie sub-basin (Y. Héroux, pers. commun., 1996). Given the structural complexity of the region, lateral variation of basement heat flux is possible, but this cannot be evaluated at a basinal scale. A basement heat flux of 110 mW/m^2 is therefore used throughout the section.

The upper boundary of the model was the sedimentation surface which is assumed to remain at constant elevation. Sedimentation rates during a specific period of time were calculated from the thicknesses of uncompacted sediments divided by the time duration. The thicknesses of uncompacted sediments are approximated by the thicknesses of the strata multiplied by 1.6, which are reduced to the thicknesses of the strata after compaction simulation. The sedimentation rates for each location (i.e., vertical grid lines in Fig. 3) of the model section, calculated for five time periods corresponding to sedimentation of the Horton, Windsor, Mabou, Cumberland, and Pictou Groups, are listed in Table 3. Unconformities are assumed to be of short duration relative to the duration of sedimentation and are not considered in the model.

The fluid overpressure and temperature at the upper boundary were maintained at zero MPa and 25°C, respectively. The center of the basin (left boundary, Fig. 3) was a symmetry plane (no flow, insulated boundary). The southern edge of the basin (right boundary, Fig. 3) was kept at hydrostatic potential and constant temperature gradient. The lower boundary of the model was the basin-basement contact which was assumed to be impermeable and heated by the specified heat flux.

The pinch-outs of the Horton Group were approximated by assigning very small thicknesses to them. Two situations were considered in the model: one is that the lower unit of the Horton Group was laterally confined by basement highs or faults, and the other is that the entire Horton Group rocks were laterally continuous throughout the basin. The pinch-outs were given evaporites permeability values for the first situation and normal (sand + shale) permeability values for the second situation. These two situations probably represent extremes which may deviate from reality; the lower part of the Horton Group may not have been regionally continuous given the horst-graben structures, neither was it completely confined due to various possible leaking processes such as hydrofracturing. Transient hydrofracturing and healing (cementation) processes (e.g., Dewers and Ortoleva, 1994) were not numerically modeled in this study due to many uncertainties regarding these processes.

Results of hydrodynamic calculations

Calculations were made for the two different Horton Group configurations outlined above: (1) the lower unit of the Horton Group was laterally confined by basement highs or faults, with the pinch-outs being given evaporite permeability values, and (2) the entire Horton Group rocks were laterally continuous throughout the basin, with the pinch-outs being given normal permeability values. In the first case, horizontal permeabilities of mixed rock types were calculated as a geometric mean, and in the second case, horizontal permeabilities were calculated as an arithmetic mean for all lithologic combinations except for the middle unit of the Windsor Group (geometric mean).

The calculation results are presented in Figures 4 to 6 and are described for the two cases described above separately.

Confined Lower Horton Group model: In this case, the pinch-outs of the lower unit of the Horton Group are given evaporite permeability values. Fluid overpressures within the lower unit of the Horton Group in the central part of the basin increased tremendously from the end of Horton sedimentation (348 Ma) to the end of Windsor sedimentation (336 Ma), slightly decreased during Mabou sedimentation (336–317 Ma), and then slightly increased during Cumberland and Pictou sedimentation (317–280 Ma; Fig. 4A). Strong

TABLE 3. Sedimentation Rates (cm/yr) during Different Periods of Time of the Maritimes Basin

Locality (grid line*)	Horton Group (367-348 Ma)	Windsor Group (348-336 Ma)	Mabou Group (336-317 Ma)	Cumberland Group (317-307 Ma)	Pictou Group (307-280 Ma)
1	2.954×10^{-2}	6.518×10^{-2}	1.137×10^{-3}	8.496×10^{-3}	1.446×10^{-3}
2	3.212×10^{-2}	5.601×10^{-2}	1.895×10^{-3}	1.318×10^{-2}	2.169×10^{-3}
3	3.468×10^{-2}	5.703×10^{-2}	2.316×10^{-3}	1.122×10^{-2}	1.446×10^{-3}
4	3.596×10^{-2}	5.601×10^{-2}	2.602×10^{-3}	1.336×10^{-2}	1.807×10^{-2}
5	3.404×10^{-2}	5.194×10^{-2}	3.183×10^{-3}	1.954×10^{-2}	2.999×10^{-3}
6	3.276×10^{-2}	4.889×10^{-2}	3.789×10^{-3}	2.622×10^{-2}	4.338×10^{-3}
7	3.043×10^{-2}	4.074×10^{-2}	4.337×10^{-3}	3.934×10^{-2}	7.230×10^{-3}
8	3.075×10^{-2}	3.258×10^{-2}	5.777×10^{-3}	4.563×10^{-2}	7.953×10^{-3}
9	2.920×10^{-2}	2.751×10^{-2}	6.939×10^{-3}	4.978×10^{-2}	8.314×10^{-3}
10	1.799×10^{-2}	4.074×10^{-2}	5.777×10^{-3}	2.514×10^{-2}	2.892×10^{-3}
11	1.285×10^{-2}	1.284×10^{-2}	3.183×10^{-3}	2.202×10^{-2}	3.615×10^{-3}
12	5.053×10^{-3}	6.678×10^{-3}	8.421×10^{-4}	8.000×10^{-4}	2.963×10^{-4}
13	2.105×10^{-2}	1.002×10^{-2}	1.154×10^{-3}	1.440×10^{-2}	2.892×10^{-3}
14	1.684×10^{-2}	9.739×10^{-3}	1.095×10^{-3}	1.120×10^{-2}	2.370×10^{-3}
15	4.211×10^{-4}	9.043×10^{-3}	1.095×10^{-3}	1.120×10^{-2}	2.370×10^{-3}

* Grid lines are counted from left to right in Figure 3

overpressures were also built up within the evaporites layer of the Windsor Group (Fig. 4A). In the sub-basin on the right side of the model, significant overpressures within the Horton and Windsor Groups were not built up until during Cumberland sedimentation (between 317 and 307 Ma), which then persisted to the end of Pictou sedimentation (280 Ma). Fluid flow was generally slow throughout the basin during the entire sedimentation history and was mainly confined in high-permeability zones, i.e., the upper unit of the Horton Group, the lower and upper units of the Windsor Group, and the Cumberland Group (Fig. 4B). Maximum horizontal and vertical fluid flow velocities (at the end of Windsor deposition) are 15.9 and 0.42 cm/yr, respectively (Fig. 4B). The temperature distribution was only slightly disturbed by fluid flow (Fig. 4B).

The evolution and distribution of fluid overpressures are further illustrated by mapping the fluid pressure/loading pressure ratios (λ) across the section (Fig. 5A). From 348 to 317 Ma, λ values are less than 1.0. High λ values approaching 1.0 are mainly distributed in the lower unit of the Horton Group and in the evaporite layer of the Windsor Group. λ values higher than 1.0 are found near the basement high and within the sub-basin during Cumberland sedimentation (between 317 and 307 Ma), which then persisted to the end of Pictou sedimentation (280 Ma). Obviously, λ values higher than 1.0 cannot be maintained for a long time, because hydrofracturing will take place when fluid pressure exceeds the least compressive stress plus the tensile strength of the rock (Hubbert and Willis, 1957). The modeling of fluid overpressure evolution including hydrofracturing requires coupled numerical solution of governing equations describing sediment compaction (fluid pressure building up) and hydrofracturing (fluid pressure dissipation) as well as sealing (fluid pressure re-building up) processes (Dewers and Ortoleva, 1994), the latter involving many physical and chemical aspects which are still not well understood. For this reason, hydrofracturing-sealing processes are not included in our model.

The contrast of fluid overpressure development in the lower unit of the Horton Group between the central part of the basin and the marginal sub-basin is highlighted by comparing their pressure-depth profiles (Fig. 6A and B). In the central part of the basin (Fig. 6A), significant fluid overpressures in the lower unit of the Horton Group were developed during Windsor sedimentation (348–336 Ma) and persisted afterward. In the marginal sub-basin (Fig. 6B), significant overpressures in the lower unit of the Horton Group, as well as fluid pressures exceeding lithostatic values in the evaporite layer of the Windsor Group, were developed during Cumberland sedimentation (317–307 Ma) and persisted afterward.

Unconfined Lower Horton Group model: When the lower unit of the Horton Group is assumed to be laterally continuous, the temperature distribution is not significantly disturbed, since in the confined model the distribution of overpressure is markedly different. As shown in Figure 5B, λ values are always lower than 1.0 (i.e., fluid pressures are lower than the loading pressures) throughout the basin during the entire sedimentation history. λ values approaching 1.0 are always found within the evaporites layer of the Windsor Group. This is more clearly illustrated in Figure 6C and D. Fluids in the Horton Group were not overpressured at all, either in the central part of the basin or in the marginal sub-basin.

Topography-Driven Flow: Model and Results

Topography-driven flow was modeled assuming that fluid overpressures due to sediment compaction had been dissipated before the establishment of the topography-driven flow system. Our model takes into account only the sub-basin south of the Cobequid highland (Figs. 1 and 3). The Cobequid highland is considered as a hydrologic divide and constitutes the left boundary of the model, i.e., fluid does not flow across this highland. The basement geometry and stratigraphy of the model is the same as the compaction model for the age of 300 Ma, but smaller spacing between vertical grid lines is used (i.e., 16 vertical grid lines spaced at 4 km apart). The boundary conditions are similar to those used in the compaction model except that hydraulic potential on the surface is set to a value corresponding to a given topographic height on the left side and gradually decreases to zero on the right side. Fluid flow velocities in a topography-driven model depend on permeabilities and the magnitude of topographic

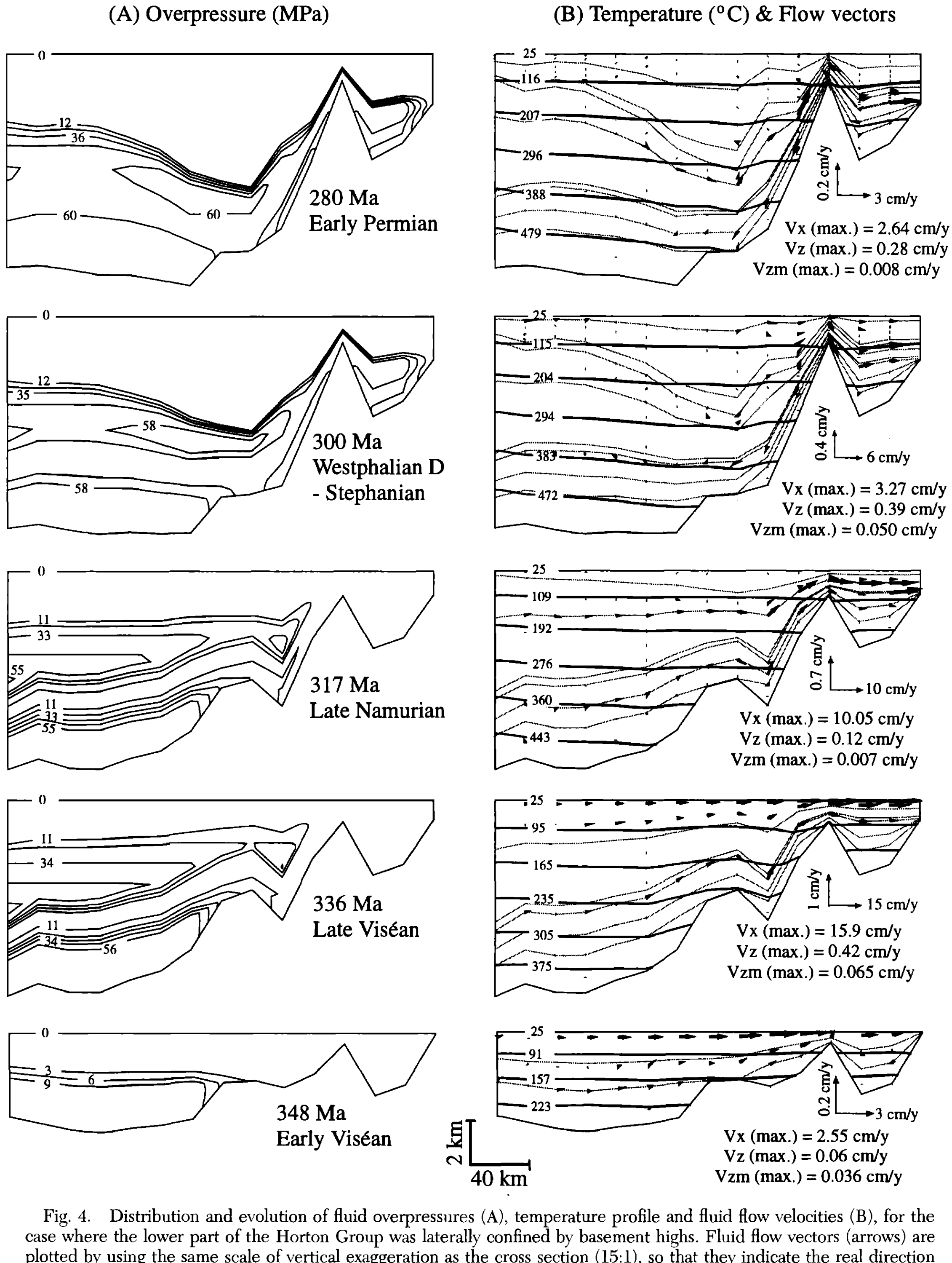

Fig. 4. Distribution and evolution of fluid overpressures (A), temperature profile and fluid flow velocities (B), for the case where the lower part of the Horton Group was laterally confined by basement highs. Fluid flow vectors (arrows) are plotted by using the same scale of vertical exaggeration as the cross section (15:1), so that they indicate the real direction of fluid flow. The maximum horizontal and vertical flow velocities (v_x and v_z) indicated in the figure have been converted from curvilinear to Cartesian coordinates. V_{zm} is the settling velocity of the solid medium.

relief (Garven and Freeze, 1984). Because none of these parameters are known here with certainty, we arbitrarily assumed a topographic relief of 750 m between the recharge area (the Cobequid highlands) and the discharge area (the Gays River deposit), and the uncertainty in fluid flow velocities was then accounted for by varying permeabilities of assumed conduits (see similar reasoning in Bethke, 1986). Also, because the uplifting rate of the Cobequids is not known with certainty, we first modeled the topography-driven flow as a steady-state problem (Garven, 1985; Bethke, 1986), and then

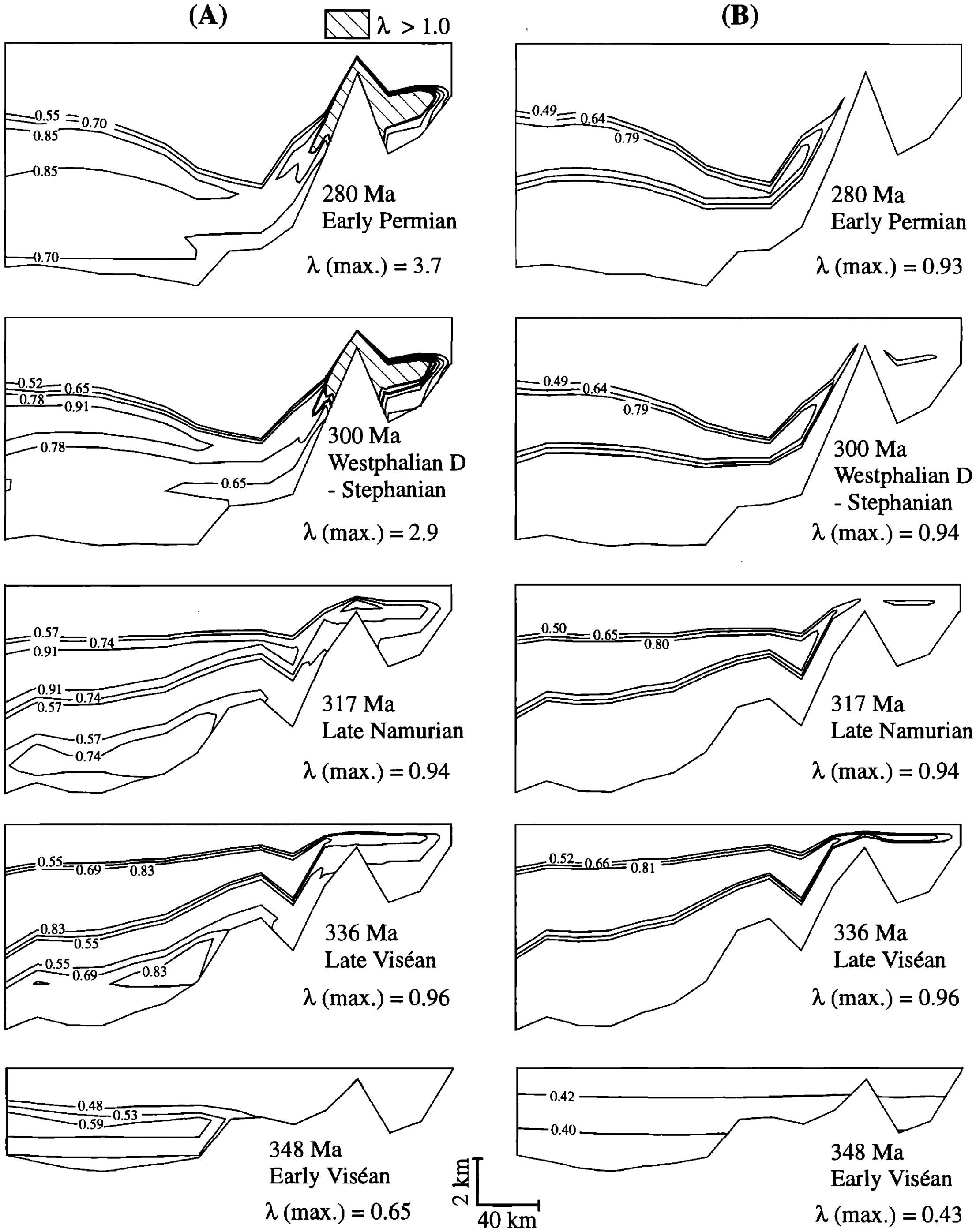

FIG. 5. Distribution and evolution of fluid pressure/loading pressure ratios (λ). Loading pressure is calculated by assuming a density of 2.3 g/cm^3 for the fluid-saturated rocks. A. The lower unit of the Horton Group is assumed to be laterally confined by basement highs. B. The lower unit of the Horton Group is assumed to be laterally continuous.

present a transient model (Garven et al., 1993). Five different permeability configurations (cases A–E, see below)have been considered with the aim to achieve optimum high temperatures in the discharge area. A basement heat flux of 110 mW/m^2, as in the compaction model, is assumed. A higher heat flux of 140 mW/m^2 (model D) has been also tried. The models and calculation results are described below.

Steady-state models

Case A: Permeability values computed in the compaction model were used without modification. This model does not consider high-permeability zones transecting strata (faults) and gives a minimum estimate of the effect of topography-driven flow on the temperature distribution. The calculation results indicate that temperature gradients near the surface

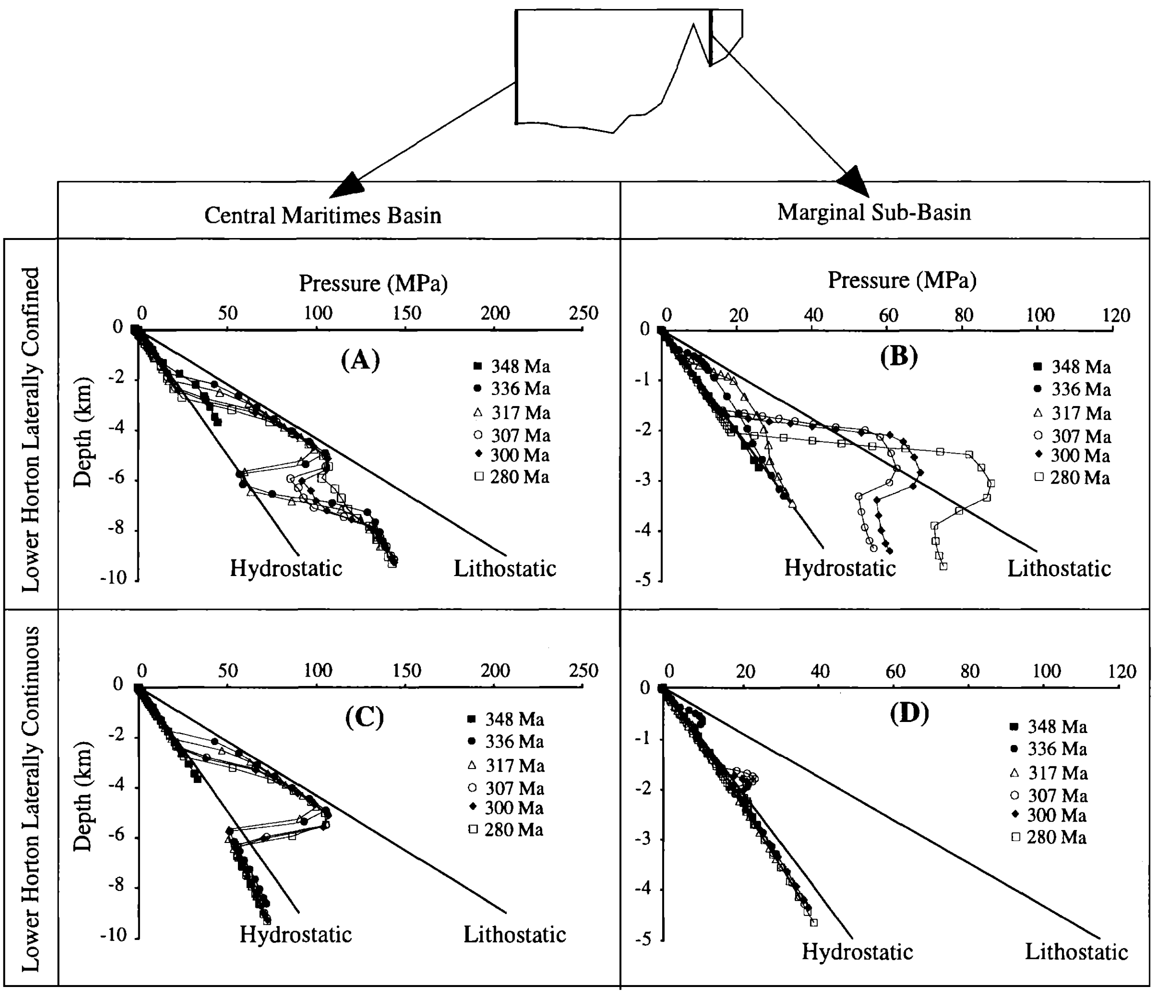

FIG. 6. Fluid pressure-depth profiles. A. In the central part of the Maritimes basin, the lower unit of the Horton Group is laterally confined by basement highs. B. In the marginal sub-basin, the lower unit of the Horton Group is laterally confined by basement highs. C. In the central part of the Maritimes basin, the lower unit of the Horton Group is laterally continuous. D. In the marginal sub-basin, the lower unit of the Horton Group is laterally continuous.

were slightly decreased (Fig. 7A) and that temperature gradients in the discharge area were also decreased (line a-a', Fig. 8A). This is probably because the hydraulic head on the surface could hardly be transmitted to the lower part of the basin due to the barrier of the evaporites layer, thus little hot fluid was driven from the deep part of the sub-basin to the discharge area.

Cases B to E: A vertical high-permeability zone (conduit) was imposed on the left two and right two (next to the right boundary) vertical grid lines of the model. These high-permeability zones cut through all stratigraphic levels from the surface to the basement contact and serve as connections between surface fluids and fluids in the Horton aquifer. This assumption of vertical high-permeability zones is based on the geologic observation that the strata in this part of the Maritimes basin are cut by a number of subvertical post-Windsor faults, but it is obviously idealized. The lower unit of the Horton Group was also given higher permeabilities to enhance lateral fluid flow.

Permeabilities assigned to the conduits and basal aquifer increase from cases B to E shown in Figure 7. In case B, the horizontal (k_x) and vertical (k_z) permeabilities of the vertical conduits are 10^{-12} and 10^{-11} cm^2 ($1\ cm^2 \approx 10^8$ D), and the k_x and k_z of the basal aquifer are 10^{-11} and 10^{-12} cm^2, respectively. The computation results indicate that temperature gradients were slightly disturbed (Fig. 7B), and the temperature at the site of mineralization (161°C) was slightly increased relative to the background temperature (150°C; line b-b', Fig. 8A). In case C, the k_x and k_z of the vertical conduits are 10^{-11} and 10^{-10} cm^2, and the k_x and k_z of the basal aquifer are 10^{-10} and 10^{-11} cm^2, respectively. The temperature gradients were slightly decreased in the recharge sector and increased in the discharge sector (Fig. 7C). The temperature at the site of mineralization (183°C) was further increased relative to case B (line c-c', Fig. 8A). In case D, the k_x and k_z values were further increased by one order of magnitude relative to case C. The geothermal gradients were significantly decreased in the recharge sector and increased toward the surface in the discharge sector (Fig. 7D). However, the temperature at the site of mineralization (175°C) was slightly decreased relative

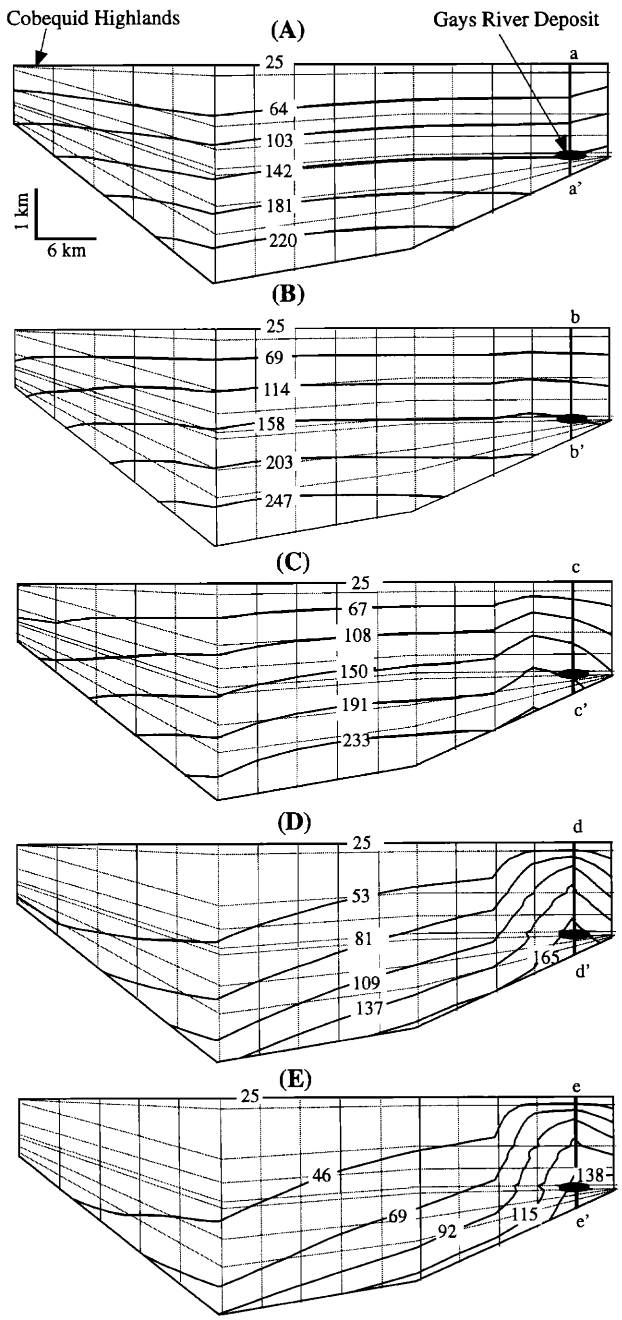

FIG. 7. Temperature distributions associated with different permeability assumptions in the topography-driven model, isotherms in °C. A hydraulic head difference of 750 m between the left and right boundarie and a basement heat flux of 110 mW/m^2, are assumed. A. Permeability values computed in the compaction model were used without modification. B. Vertical high-permeability zone, with horizontal and vertical permeabilities (k_x and k_z) of 10^{-12} and 10^{-11} cm^2, respectively, was imposed on the left two and right two (next to the right boundary) vertical grid lines of the model, and the lower unit of the Horton Group was also given high permeabilities, with k_x and k_z being set at 10^{-11} cm^2 and 10^{-12} cm^2, respectively. C. The k_x and k_z of the vertical conduits are 10^{-11} and 10^{-10} cm^2, and the k_x and k_z of the basal aquifer are 10^{-10} and 10^{-11} cm^2, respectively. D. The k_x and k_z of the vertical conduits are 10^{-10} and 10^{-9} cm^2, and the k_x and k_z of the basal aquifer are 10^{-9} and 10^{-10} cm^2, respectively. E. The k_x and k_z of the vertical conduits are 10^{-10} and 10^{-8} cm^2, and the k_x and k_z of the basal aquifer are 10^{-8} and 10^{jims10} cm^2, respectively. The vertical lines a-a', b-b', c-c', d-d', and e-e' indicate the position of the depth-temperature profile shown in Figure 8.

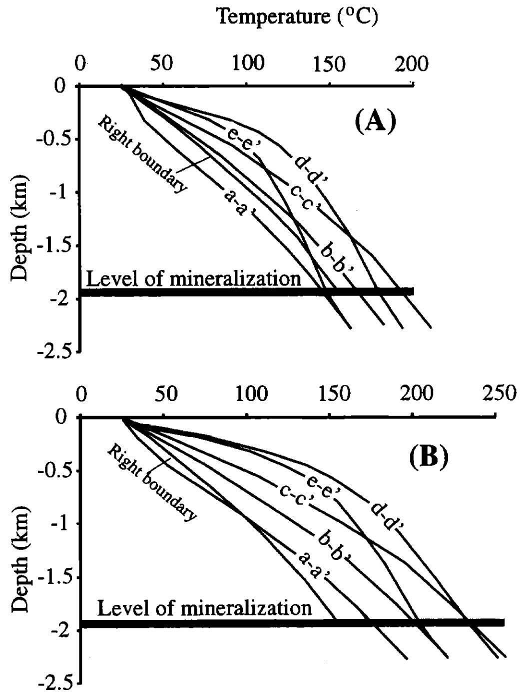

FIG. 8. Temperature-depth profiles for lines a-a', b-b', c-c', d-d' and e-e' shown in Figure 7. A. Basement heat flux is assumed to be 110 mW/m^2. B. Basement heat flux is assumed to be 140 mW/m^2.

to case C (line d-d', Fig. 8A). In case E, the k_x and k_z of the vertical conduits are 10^{-10} and 10^{-8} cm^2, and the k_x and k_z of the basal aquifer are 10^{-8} and 10^{-10} cm^2, respectively. The geothermal gradients were decreased in the recharge sector as well as in the discharge sector (Fig. 7E). The temperature at the site of mineralization (145°C) was significantly decreased relative to case D (line e-e', Fig. 8A).

Cases A' to E': The same permeability configurations as cases A to E have been used, but a higher basement heat flux of 140 mW/m^2 is assumed across the basin except on the right boundary. The heat flux on the right boundary remains the same as in cases A to E and serves to indicate the background thermal condition. The assumption of a heat flux of 140 mW/m^2 is based on data from the vertical variation of vitrinite reflectance (R_o) values along a deep drill core in the center of the Shubenacadie sub-basin north of Gays River, which indicates a geothermal gradient of at least 80°C/km (Y. Héroux, pers. commun., 1996). This geothermal gradient is extremely high and may be of only local significance. We use it here merely to give an upper limit to the steady-state topography-driven model. The computation results show similar temperature patterns as in cases A to E, but the temperatures are shifted to higher values relative to the background geothermal gradient defined on the basis of a 110 mW/m^2 heat flux (see Fig. 8B). With this high heat flux assumption, the temperature near the level of mineralization can be close to 230°C.

In addition to the above variational studies, we have also tried to give the Horton Group a larger thickness (max 3.5 km according to stratigraphic data of Murphy et al., 1994, for the Saint Mary's sub-basin). It is noted that the temperatures obtained at the site of mineralization were only a few degrees higher than in the above models.

From the above calculation results it is shown that under steady-state conditions, topography-driven flow could elevate the geothermal gradients in the discharge area if high-permeability zones (conduits) linking the highlands, basal aquifer, and the discharge area are assumed. However, under the same basement heat flux assumption used for the compaction models (110 mW/m^2), the temperature at the site of mineralization could not be higher than 185°C. A further increase in the permeability of the conduits (or increase in topographic relief) cannot increase the temperature in the discharge area. This is because imposing high-permeability zones has a two-sided effect on temperature distribution. On one hand, an increase in fluid flow velocities due to higher permeabilities helps to bring hot fluids from deep to shallow parts of the basin by minimizing heat loss due to thermal conduction. On the other hand, an increase in fluid flow velocities brings cool fluids from the surface to deep parts of the basin, and thus lowers the temperature of the fluids in the deep parts of the basin. Similar observations have been reported by Garven and Freeze (1984), Garven (1985), and Bethke (1986).

Transient models

The same physical models as cases A to E above are used to simulate the temporal variation of temperature. Two situations were modeled: (1) the Cobequid highlands were uplifted to the height of 750 m instantaneously, and (2) that the highlands were rising at a rate of 1 mm/yr. Figure 9A shows the variation of temperature at the site of mineralization assuming instantaneous uplifting of the Cobequids. It is shown that for cases A, B, and C, the temperature gradually increases

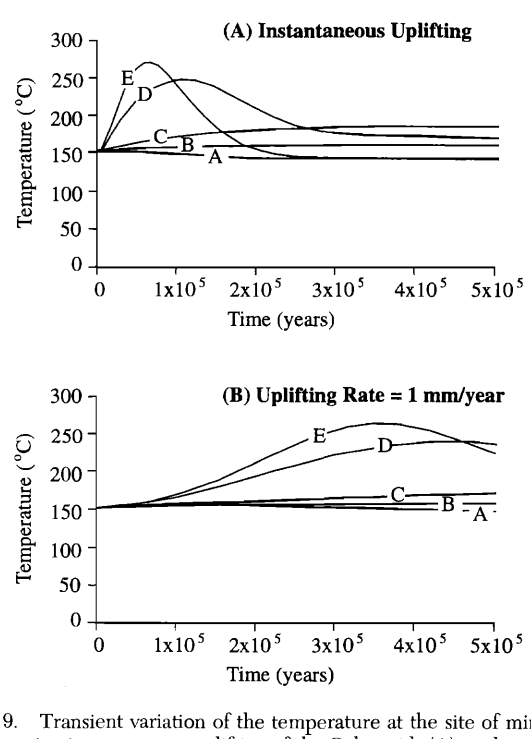

FIG. 9. Transient variation of the temperature at the site of mineralization, assuming instantaneous uplifting of the Cobequids (A), and an uplifting rate of 1 mm/yr (B).

toward the steady-state value. In the cases of D and E, i.e., when the maximum permeability in the vertical conduits and basal aquifer is 10^{-9} and 10^{-8} cm^2 (0.1 and 1 D), the temperature rapidly increases from the background value to a peak of about 250° and 270°C, respectively, and then gradually decreases toward the steady-state value. When an uplifting rate of 1 mm/yr is assumed (Fig. 9B), the temperature peaks are slightly lowered and are widened; transient high temperatures were reached later and lasted longer than in the case of instantaneous uplifting.

Discussion: Implications on Fluid Sources and Driving Forces

A major constraint on the sources and driving forces of the ore-forming fluids is the fluid temperatures inferred from fluid inclusion studies. Homogenization temperatures (T_h) of fluid inclusions from the deposits are highly variable, e.g., 50° to 230°C for the Jubilee deposit (Chi et al., 1995a), 50° to 260°C for the Gays River deposit (Ravenhurst et al., 1989; Kontak, 1992, 1998; Chi and Savard, 1995), and 100° to 320°C for the Walton deposit (Kontak and Sangster, 1998). These variations in T_h have been interpreted to have resulted from mixing between fluids with high and low temperatures, and the high-temperature end members (ca. 250°C, for the convenience of discussion) were most likely the metal-carrying fluids (Chi and Savard, 1995; Chi et al., 1995a). The validity of the high T_h values is supported, in the case of the Gays River deposit, by vitrinite reflectance data (Héroux et al., 1994) which indicate that the host rock was heated to 230°C, and by the partial resetting of the $^{40}Ar/^{39}Ar$ isotope system at ca. 300 Ma, which indicates temperatures between 250° and 300°C (Kontak et al., 1994). Clearly, the ore-forming fluids were derived from source regions where temperatures were much higher than those in the sites of mineralization, and an efficient driving force must have advected these hot fluids at a sufficient speed to compensate for heat loss due to thermal conduction and to preserve the high fluid temperatures.

Ravenhurst and Zentilli (1987) and Ravenhurst et al. (1989), based on the assumption that the geothermal gradient near the time of mineralization was about 45° to 55°C/km, suggested that the ore-forming fluids were derived from the central part of the Maritimes basin, which is at least 100 to 150 km away from the sites of mineralization. However, as indicated by Chi et al. (1998), the paleogeothermal gradients near the time of mineralization were very likely higher than 65°C/km. Consequently, temperatures higher than those recorded by fluid inclusions in the deposits may have been reached in deep parts of the sub-basins not far from the sites of mineralization. For example, with a thermal gradient of 65°C/km, a temperature of 250°C can be reached at a depth of only 3.5 km (assuming a surface temperature of 25°C). Such conditions can be reached in many sub-basins in the southern margin of the Maritimes basin. Isotopic studies (Savard and Kontak, 1998; Sangster et al., 1998) and fluid inclusion studies (Chi et al., 1998; Savard and Chi, 1998) suggest that the ore-forming fluids for different deposits were derived from distinct source regions, most likely from nearby sub-basins.

With the ore-forming fluids being associated with proximal sub-basins, the difficulty with the distal model, i.e., maintaining overpressures to drive fluids over a long distance (>100 km), is minimized. The problem that remains is whether the hot fluids in the sub-basins could be advected to the sites of mineralization without a significant decrease in temperature. Fluid flow driven by sediment compaction has been shown to be too slow to disturb the temperature profile significantly. Two possible mechanisms are topography-driven flow related to the highlands and sudden release of overpressured fluids from the sub-basins, which are discussed below. Other possibilities, e.g., heat anomaly-induced fluid circulation and fluid penetration into the basement, have not been considered.

The numerical modeling of topography-driven flow indicates that the temperature distribution in the sub-basin was only slightly disturbed if rock permeabilities were inherited from sediment compaction. If high-permeability zones could be established by some process such as faulting, which serves to break through the low-permeability evaporite layer of the Windsor Group and to connect the lower Horton aquifer with the recharge and discharge areas on the surface, then geothermal gradients in the discharge area could be increased. If the permeabilities of the assumed vertical conduits and the basal aquifer are higher than 0.1 D, the temperature at the site of mineralization could be transiently elevated to values indicated by fluid inclusions (ca. 250°C). Clearly, the functioning of the topography-driven model depends strongly on the assumption of high-permeability zones. Although it is known that many subvertical faults cut through the Windsor evaporites, it is uncertain whether the high permeabilities assumed for the vertical conduits and basal aquifer could have existed at the time of mineralization.

The numerical modeling of overpressure development indicates that, as the Horton Group sediments were laterally confined by basement highs or faults, fluid pressures approaching or exceeding loading pressures could have been built up within the Horton Group, not only in the central part of the Maritimes basin but also in shallower sub-basins close to the sites of mineralization. Although fluid pressures exceeding lithostatic loads (i.e., λ values higher than 1.0) represent extreme conditions and must have been episodically released, fluid pressures approaching lithostatic values were likely to have existed in the basal part of the marginal sub-basins. These overpressured fluids, if suddenly released through hydrofracturing or by a tectonic event, could be focused toward the sites of mineralization (Sharp, 1978). Considering the short distance between the source regions and the sites of mineralization (ca. 30 km or less), and the outburst nature of the fluid flow, hot fluids in the deep parts of the sub-basins could have been brought to the basin edge with minimum heat loss.

Based on the numerical modeling results, although other models cannot be completely excluded, we favor sudden release of overpressured fluids from the deep parts of sub-basins proximal to the deposits as the fluid flow mechanism responsible for mineralization (the proximal source-overpressure model), a process similar to that proposed by Fowler and Anderson (1991). A two-stage fluid flow scenario, i.e., an overpressure-driven fluid flow in the main stage of mineralization followed by topography-driven flow in the postmineralization stage, as proposed by Chi et al. (1995b), may be envisaged.

Outburst of overpressured fluids may have been provoked by a tectonic event, which could also have created structures to focus fluid flow. The age of mineralization of the Gays River deposit (ca. 300 Ma or between 300 and 320 Ma) broadly coincides with a period of relatively intensive deformation of the region, as indicated by the unconformity between the Cumberland and the Pictou Groups (ca. 307 Ma). A number of subvertical faults north of the Gays River deposit (Giles and Boehner, 1982), which cut through the strata of the Windsor and Horton Groups, as well as the Canso (Mabou) Group, were probably developed during this period of time. On Cape Breton Island, large-scale detachment faulting probably took place at about the same time (or slightly earlier). Lynch and Brisson (1994) proposed that detachment faulting prompted overpressure-driven fluid flow by unloading covering strata and by creating high-permeability zones in the basal carbonate unit of the Windsor Group.

The overpressured fluids in the lower unit of the Horton Group (the major metal carrier) could have been conveyed rapidly to the sites of mineralization through different combinations of paths. They could have first breached the confining layer of the Middle Horton Group through hydrofracturing and/or faulting along some subvertical faults, and then flowed laterally to the sites of mineralization along some high-permeability zones in the basal carbonate unit of the Windsor Group. Alternatively, they may have first migrated laterally toward the sites of mineralization within the lower Horton, and then been channeled upward along subvertical faults at or near the deposit. Fluids coming from different stratigraphic levels with different temperature and composition may have been focused toward the sites of mineralization and mixed, as indicated by fluid inclusion and isotopic data (Chi and Savard, 1995; Chi et al., 1995a; Kontak and Sangster, 1998; Savard and Kontak, 1998).

After the dissipation of fluid overpressures, the basal aquifer may have been connected to the surface through fractures produced during the outburst, and topography-driven flow may have been dominant and responsible for fluid circulation in the postore stage. It has been noticed that a fluid with lower salinity and temperature was involved in the hydrothermal system after the main-stage mineralization in the Jubilee and Gays River deposits (Chi and Savard, 1995; Chi et al., 1995a). This late fluid was probably part of the topography-driven system.

Conclusions

The objective of this paper has been to evaluate mechanisms of basinal fluid flow responsible for Zn-Pb mineralization on the southern margin of the Maritimes basin. The major conclusions are the following:

1. Fluid pressures approaching or exceeding loading pressures could have been built up within the lower unit of the Horton Group when it was laterally confined by basement highs or faults. This overpressuring could take place not only in the central part of the Maritimes basin but also in sub-basins close to the deposits. Overpressured fluids in the basal part of the proximal sub-basins would provide a potential

source of mineralizing fluids, which could be suddenly released through tectonic events. The short distance between the proposed source regions and the sites of mineralization would minimize temperature decrease during fluid migration, and high fluid temperatures (ca. 250°C) as recorded by fluid inclusions could have been reached at the deposits.

2. Topography-driven flow related to uplifting of highlands could increase the geothermal gradients in the discharge area if high-permeability zones penetrating the evaporites layer and connecting the basal aquifer with the surface were established. The temperature at the site of mineralization could be transiently elevated to those indicated by fluid inclusions if permeabilities in the vertical conduits and the basal aquifer were higher than about 0.1 D. The validity of topography-driven flow depends strongly on the assumption of high-permeability zones and needs further study. Sudden release of overpressured fluids from proximal sub-basins is considered as the more likely mechanism responsible for mineralization. Topography-driven flow may have been dominant after the dissipation of overpressures and may have been responsible for fluid flow in the postore stage.

Acknowledgments

This study was financially supported by the Canada-Nova Scotia Cooperation Agreement on Mineral Development (1992–1996). We thank R. Lefebvre for helpful discussion in hydrogeology and numerical modeling techniques and for reviewing the manuscript, and P. Giles, D. Lavoie, M.R. Gibling, B. Murphy, Y. Héroux, and D.F. Sangster for stimulating discussions. We are grateful to D.F. Sangster and *Economic Geology* reviewers G. Garven and A.D. Fowler for their critical and constructive review of the manuscript.

REFERENCES

Bethke, C.M., 1985, A numerical model of compaction-driven groundwater flow and heat transfer and its application to the paleohydrology of intracratonic sedimentary basins: Journal of Geophysical Research, v. 90, p. 6817–6828.

——1986, Hydrologic constraints on the genesis of the Upper Mississippi Valley mineral district from Illinois basin brines: ECONOMIC GEOLOGY, v. 81, p. 233–249.

Chatterjee, A.K., and Muecke, G.K., 1982, Geochemistry and the distribution of uranium and thorium in the granitoid rocks of the South Mountain batholith, Nova Scotia: Some genetic and exploration implications: Geological Survey of Canada Paper 81–23, p. 11–17.

Chi, G., and Savard, M.M., 1995, Fluid evolution and mixing in the Gays River carbonate-hosted Zn-Pb deposit and its surrounding barren areas, Nova Scotia: Atlantic Geology, v. 31, p.141–152.

Chi, G., Savard, M.M., and Héroux, Y., 1995a, Constraints from fluid-inclusion data on the origin of the Jubilee carbonate-hosted Zn-Pb deposit, Cape Breton, Nova Scotia: The Canadian Mineralogist, v. 33, p. 709–721.

Chi, G., Savard, M.M., St.-Antoine, P., and Héroux, Y., 1995b, Basinal fluid flow mechanisms related to carbonate-hosted Zn-Pb mineralization in the Maritimes basin, Nova Scotia, Canada—an overview[abs.]: Geological Society of America Abstracts with Programs, v. 27, no. 6, p. A378.

Chi, G., Kontak, D.J., and Williams-Jones, A.E., 1998, Fluid composition and thermal regime during Zn-Pb mineralization in the Lower Windsor Group, Nova Scotia, Canada: ECONOMIC GEOLOGY, v. 93, p. 883–895.

Dewers, T., and Ortoleva, P., 1994, Nonlinear dynamical aspects of deep basin hydrology: Fluid compartment formation and episodic fluid release: American Journal of Science, v. 294, p. 713–755.

Durling, P., and Marillier, F., 1993, Tectonic setting of Middle Devonian to lower Carboniferous rocks in the Magdalen basin: Atlantic Geology, v. 29, p. 199–217.

Fowler, A.D., and Anderson, M.T., 1991, Geopressure zones as proximal sources of hydrothermal fluids in sedimentary basins and the origin of Mississippi Valley type deposits in shale rich sequences: Institute of Mining and Metallurgy Transactions, v. 100, p. B14–B18.

Garven, G., 1985, The role of regional fluid flow in the genesis of the Pine Point deposit, Western Canada sedimentary basin: ECONOMIC GEOLOGY, v. 80, p. 307–324.

Garven, G., and Freeze, R. A., 1984, Theoretical analysis of the role of groundwater flow in the genesis of stratabound ore deposits. 2. Quantitative results: American Journal of Science, v. 284, p. 1125–1174.

Garven, G., Ge, S., Person, M.A., and Sverjensky, D.A., 1993, Genesis of stratabound ore deposits in the midcontinent basins of North America. 1. The role of regional groundwater flow: American Journal of Science, v. 293, p. 497–568.

Giles, P.S., and Boehner, R.C., 1982, Geological map of the Shubenacadie and Musquodoboit basins, central Nova Scotia: Nova Scotia Department Mines and Energy Map 82–4, scale 1:50,000.

Graves, M.C., and Hein, F.J., 1994, Compilation, synthesis, and stratigraphic framework of mineral deposits within the basal Windsor Group, Atlantic Provinces, Canada: Geological Survey of Canada Open File 2914, 485 p.

Hacquebard, P.A., 1986, The Gulf of St. Lawrence Carboniferous basin: The largest coalfield of eastern Canada: Canadian Institute of Mining and Metallurgy Bulletin, v. 79, no. 891, p. 67–78.

Hamblin, A.P., 1992, Half-graben lacustrine sedimentary rocks of the lower Carboniferous Strathlorne Formation, Horton Group, Cape Breton Island, Nova Scotia, Canada: Sedimentology, v. 39, p. 263–284.

Harrison, W.J., and Summa, L.L., 1991, Paleohydrology of the Gulf of Mexico basin: American Journal of Science, v. 291, p. 109–176.

Héroux, Y., Chagnon, A., and Savard, M.M., 1994, Anomalies des propriétés de la matière organique et des assemblages argileux associés au gîte de Pb-Zn de Gays River, Nouvelle-Écosse, Canada: Exploration and Mining Geology, v. 3, p. 67–79.

Howie, R.D., and Barss, M.S., 1975, Upper Paleozoic rocks of the Atlantic Provinces, Gulf of St. Lawrence, and adjacent continental shelfs: Geological Survey of Canada Paper 74–30, p. 35–50.

Hubbert, M.K., and Willis, D.G., 1957, Mechanics of hydraulic fracturing: American Institute of Mining, Metallurgical, and Petroleum Engineers, Society of Petroleum Engineers Transactions, v. 210, p. 153–166.

Jaluria, Y., and Torrance, K.E., 1986, Computational heat transfer: Hemisphere Publishing Corporation, 366 p.

Kakac, S., and Yener, Y., 1985, Heat conduction, 2nd ed.: Hemisphere Publishing Corporation, 397 p.

Kaufman, J., 1994, Numerical models of fluid flow in carbonate platforms: Implications for dolomitization: Journal of Sedimentary Research, v. A64, p. 128–139.

Keppie, J.D., 1982, The Minas geofracture: Geological Association of Canada Special Paper 24, p. 263–280.

Kontak, D.J., 1992, A preliminary report on geochemical, fluid inclusion and isotopic studies of the Gays River Zn-Pb deposit, Nova Scotia: Nova Scotia Department of Natural Resources Open File Report 92–014, 223 p.

——1998, A study of fluid inclusions in ore and gangue mineral phases from a carbonate-hosted Zn-Pb deposit, Gays River, Nova Scotia: ECONOMIC GEOLOGY, v. 93, p. 793–817.

Kontak, D.J., and Sangster, D.F., 1998, Aqueous and liquid petroleum inclusions in barite from the Walton, Nova Scotia, Canada: A Carboniferous, carbonate-hosted Ba-Zn-Pb-Cu-Ag: ECONOMIC GEOLOGY, v. 93, p. 845–868.

Kontak, D.J., McBride, S.L., and Farrar, E., 1994, $^{40}Ar/^{39}Ar$ dating of fluid migration in a Mississippi-Valley type deposit: Gays River Zn-Pb deposit, Nova Scotia: ECONOMIC GEOLOGY, v. 89, p. 1501–1517.

Lavoie, D., 1994, Lithology and preliminary paleoenvironmental interpretation of the Macumber and Pembroke formations (Windsor Group, Early Carboniferous), Nova Scotia: Geological Survey of Canada, Current Research, Paper 1994-D, p. 79–88.

Lynch, G., and Brisson, H., 1994, Ainslie detachment in the Carboniferous River Denys basin of Cape Breton Island, Nova Scotia, with regional implications for Pb-Zn mineralization: Geological Survey of Canada, Current Research, Paper 1994-D, p. 57–62.

Lynch, G., and Tremblay, C., 1994, Late Devonian-Carboniferous detachment faulting and extensional tectonics in western Cape Breton Island, Nova Scotia, Canada: Tectonophysics, v. 238, p. 55–69.

Martel, A.T., and Gibling, M.R., 1996, Stratigraphy and tectonic history of the Upper Devonian to lower Carboniferous Horton Bluff Formation, Nova Scotia: Atlantic Geology, v. 32, p. 13–38.

Murphy, J.B., Stokes, T.R., Meagher, C., and Mosher, S.-J., 1994, Geology

of eastern St. Mary's basin, central mainland Nova Scotia: Geological Survey of Canada, Current Research, Paper 1994-D, p. 95–102.
Pan, H., Symons, D.T.A., and Sangster, D.F., 1993, Palaeomagnetism of the Gays River zinc-lead deposit, Nova Scotia: Pennsylvannian ore genesis: Geophysical Research Letters, v. 20, p. 1159–1162.
Phillips, S.L., Igbene, A., Fair, J.A., and Ozbek, H., 1981, A technical databook for geothermal energy utilization: Lawrence Berkeley Laboratory Report, LBL-12810, 46 p.
Raffensperger, J.P., and Garven, G., 1995, Fluid flow and geochemical modeling in sediment: International Field Conference on Carbonate-Hosted Lead-Zinc Deposits, Pre-Conference Workshop A, St. Louis, Missouri, June 2, 1995, Short Course Notes, 127 p.
Ravenhurst, C.E., and Zentilli, 1987, A model for the evolution of hot (>200°C) overpressured brines under an evaporite seal: The Fundy/Magdalen Carboniferous basin of Atlantic Canada and its associated Pb-Zn-Ba deposits: Canadian Society of Petroleum Geologists Memoir 12, p. 335–349.
Ravenhurst, C.E., Reynolds, P.H., Zentilli, M., Krueger, H.W., and Blenkinsop, J, 1989, Formation of Carboniferous Pb-Zn and barite mineralization from basin-derived fluids, Nova Scotia, Canada: ECONOMIC GEOLOGY, v. 84, p. 1471–1488.
Reed, B.C., Nance, R.D., Calder, J.H., and Murphy, J.B., 1993, The Athol syncline: Tectonic evolution of a Westphalian A-B depocentre in the Maritimes basin, Nova Scotia: Atlantic Geology, v. 29, p. 179–186.
Ryan, R.J., and Boehner, R.C., 1994, Geology of the Cumberland basin, Cumberland, Colchester, and Pictou Counties, Nova Scotia: Nova Scotia Department of Natural Resources, Mines and Energy Branches Memoir 10, 222 p.
Ryan, R.J., Boehner, R.C., and Calder, J.H., 1991, Lithostratigraphic revisions of the upper Carboniferous to Lower Permian strata in the Cumberland basin, Nova Scotia and the regional implications for the Maritimes basin in Atlantic Canada: Canadian Petroleum Geology Bulletin, v. 39, p. 289–314.
Sangster, D.F., and Savard, 1994, Fluid migration and mineralization in the Lower Windsor Group, Nova Scotia. 12. Summary and conclusions [abs.]: Nova Scotia Department of Natural Resources, 18th Annual Review of Activities, Program and Summaries, p. 57.
Sangster, D.F., Savard, M.M., and Kontak, D.J., 1998, Sub-basin-specific Pb and Sr sources of Pb-Zn deposits of the Lower Windsor Group, Nova Scotia: ECONOMIC GEOLOGY, v. 93, p. 911–919.
Savard, M.M., and Chi, G., 1998, Cation study of fluid inclusion decrepitates in the Jubilee and Gays River Zn-Pb deposits—characterization of ore-forming brines: ECONOMIC GEOLOGY, v. 93, p. 920–931.
Savard, M.M., and Kontak, D.J., 1998, $\delta^{13}C$-$\delta^{18}O$-$^{87}Sr/^{86}Sr$ covariations in ore-stage calcites at and around the Gays River (Canada) Pb-Zn deposit: Evidence for fluid mixing: ECONOMIC GEOLOGY, v. 93, p. 818–833.
Sharp, J.M., Jr., 1978, Energy and momentum transport model of the Ouachita basin and its possible impact on formation of economic mineral deposits: ECONOMIC GEOLOGY, v. 73, p. 1057–1068.
St. Peter, C., 1993, Maritimes basin evolution: Key geologic and seismic evidence from the Moncton Subbasin of New Brunswick: Atlantic Geology, v. 29, p. 233–269.

APPENDIX

The fluid flow and heat transfer processes during sedimentation and compaction are described by the following three equations according to the mathematical model of Bethke (1985):

Medium continuity:

$$\frac{\partial v_{zm}}{\partial z} = \frac{1}{(1-\phi)}\frac{\partial \phi}{\partial t} \quad \text{(A1)}$$

Fluid flow continuity:

$$\phi\beta\frac{\partial \Phi}{\partial t} - \frac{1}{\rho}\left[\frac{\partial}{\partial x}\left(\frac{\rho k_x}{\mu}\frac{\partial \Phi}{\partial x}\right) + \frac{\partial}{\partial z}\left(\frac{\rho k_z}{\mu}\frac{\partial \Phi}{\partial z}\right)\right] = -\phi\beta\rho g v_{zm} - \frac{1}{(1-\phi)}\frac{\partial \phi}{\partial t} + \phi\alpha\frac{\partial T}{\partial t} \quad \text{(A2)}$$

Heat conservation:

$$[\rho\phi C_f + \rho_r(1-\phi)C_r]\frac{\partial T}{\partial t} - \frac{\partial}{\partial x}\left(K_x\frac{\partial T}{\partial x}\right) + \frac{\partial}{\partial z}\left(K_z\frac{\partial T}{\partial z}\right) + \frac{\partial}{\partial x}(\rho v_x h_f) + \frac{\partial}{\partial z}(\rho v_z h_f) = -h_f\frac{\partial}{\partial t}(\rho\phi) \quad \text{(A3)}$$

where v_{zm} is settling velocity of the medium, z is the vertical coordinate, x the horizontal coordinate, t is time, ϕ is porosity, Φ is fluid overpressure, which is defined by:

$$\Phi = P - \rho g z \quad \text{(A4)}$$

P is fluid pressure, ρ is fluid density, g is gravity, k_x and k_z are intrinsic permeabilities in x and z directions, K_x and K_z are thermal conductivities in and z directions, is temperature, v_x and v_z are fluid velocities in x and z directions, h_f is fluid enthalpy. Other symbols used in the equations are explained in Table 1. Details about the derivation of the equations can be found in Bethke (1985, 1986). It must be mentioned here that the equations were derived in a Lagrangian reference frame, which remains fixed with respect to the subsiding medium but moves through space. The term "overpressure" used in this study is equivalent to "hydraulic potential" used by Bethke (1985, 1986). A discussion about the definition of hydraulic potential can be found in Harrison and Summa (1991).